Fault Tolerant Path Following for a Quadrotor

Adeel Akhtar, Steven L. Waslander, Christopher Nielsen

***Abstract*— This paper presents a path following controller for a quadrotor UAV experiencing a single rotor failure. A smooth, dynamic feedback control law is proposed that allows the quadrotor to follow both closed and non-closed embedded curves while maintaining a desired velocity profile along the path when one out of four motors is completely disabled due to failure. The nonlinear model of the quadrotor is transformed into a partially linear model by a coordinate and feedback transformation. A path following controller is designed for transformed system that guarantees invariance of the path. The uncontrolled nonlinear portion of the dynamics (internal dynamics) are shown to be bounded.**

I. Introduction

A quadrotor is an aerial mobile robot with a four rotor setup in a cross configuration. Many indoor applications exist for the quadrotor, which require reliable operation in cluttered environments. In such a scenario, the quadrotor needs to follow a given path precisely in order to avoid obstacles. However, due to unknown disturbances and uncertainties in the environment, there exists the possibility that one of the rotors of a quadrotor come in contact with an obstacle. Such accidents can cause a large imbalance in the body torques and typical controllers may result in loss of the vehicle, or in an extreme case, collision with a human being.

The dynamics of the quadrotor vehicle are nonlinear and various works have proposed nonlinear controllers for fault free stabilization. Feedback linearization [1]–[3] and backstepping [4] are the most commonly used techniques, and have both been implemented and demonstrated in flight in nominal hover conditions.

Most of the controllers presented for quadrotors are trajectory tracking controllers. In [5] the authors present a path following controller for a fault free quadrotor system. The path following controller provides certain advantages such as path invariance, ensuring that once the system gets on the path it will stay on the path for all future time, which is beneficial when working in close proximity to obstacles.

Compared to the fault free case, less research has been done for fault tolerant control of quadrotors. In [6], [7] the authors propose a fault tolerant controller for quadrotors using sliding mode control. In [8] the authors proposed a fault tolerant controller based on trajectory linearization when one rotor of the quadrotor fails. In [9] the authors applied feedback linearization and discussed the problem of trajectory tracking by following the inner-outer loop control structure.

In this work, a path following controller is proposed for the case when one rotor of the quadrotor encounters a failure. The control design process is challenging because it requires the controller to manage six degrees of freedom using only three control inputs instead of four. It is shown in this work that using fault tolerant path following, the system can be made to stay precisely on the path, in other words path invariance can be achieved while the quadrotor is running only on three rotors. Unlike the previous work for the case of fault free system [5] where the system was shown to be differentially flat, the three rotor system is not differentially flat, but instead presents uncontrolled internal dynamics. Nonetheless, it is shown that the vehicle is still able to follow the given path, maintain the desired speed along the path, and does not rotate at an unbounded rate.

1) Notation: The point-to-set distance from a point $x \in \mathbb{R}^m$ to a set $\Gamma \subset \mathbb{R}^n$ is denoted by $\|x\|_\Gamma := \inf_{p\in\Gamma} \|x - p\|$ where $\|\cdot\|$ is the Euclidean norm. Given two vectors $x, y \in \mathbb{R}^n$ the inner product is denoted by $\langle x, y\rangle$ and, when $n = 3$, the vector (cross) product is denoted by $x \times y$. Trigonometric functions are abbreviated as $S_i := \sin(x_i)$, $C_i := \cos(x_i)$ and $T_i := \tan(x_i)$. Let $\mathrm{col}(x_i, \ldots, x_k) := \begin{bmatrix} x_i & \cdots & x_k \end{bmatrix}^\top$ where $^\top$ denotes transpose. Given a C^1 map $f : \mathbb{R}^n \to \mathbb{R}^m$ and a point $p \in \mathbb{R}^n$, the Jacobian of f evaluated at p is denoted df_p. If $f, g : \mathbb{R}^n \to \mathbb{R}^n$ and $\lambda : \mathbb{R}^n \to \mathbb{R}$ are smooth, we use the following standard notation for iterated Lie derivatives $L_g^0\lambda := \lambda$, $L_g^k\lambda := L_g(L_g^{k-1}\lambda)$, $L_gL_f\lambda := L_g(L_f\lambda)$.

II. Dynamic model of the quadrotor

A fault free quadrotor is a nonlinear unmanned aerial vehicle (UAV) consisting of four actuators, i.e., four motors with rotors attached. Two diagonal motors M_1 and M_3 rotate in one direction while the other two M_2 and M_4 rotate in the opposite direction. Because of this configuration the gyroscopic effects and aerodynamic effects tend to balance each other. The inertial and body frames are represented, respectively, by $\mathcal{I}$ and $\mathcal{B}$. Let $\chi := \mathrm{col}(x_I, y_I, z_I) \in \mathbb{R}^3$ and $\dot\chi := \mathrm{col}(\dot x_I, \dot y_I, \dot z_I) \in \mathbb{R}^3$ represent, respectively, the position and velocity of a quadrotor in the frame $\mathcal{I}$. The attitude of the quadrotor is represented by the Euler angles $\Omega := \mathrm{col}(\phi, \theta, \psi) \in \mathbb{R}^3$. Let the body rates be represented as $\omega := \mathrm{col}(p, q, r) \in \mathbb{R}^3$. For a detailed discussion on quadrotor modelling, the reader is referred to [9]–[11]. Let the state vector of the quadrotor be $x := \mathrm{col}(x_1, \ldots, x_{12}) = \mathrm{col}(\Omega, \omega, \chi, \dot\chi) \in \mathbb{R}^{12}$. It is shown in [9] that using an Euler-Lagrange approach, the state space model of the quadrotor

Supported by the Natural Sciences and Engineering Research Council of Canada (NSERC).

A. Akhtar and S. Waslander are with the Department of Mechanical and Mechatronics Engineering and C. Nielsen is with the Department of Electrical and Computer Engineering, University of Waterloo, 200 University Avenue West, Waterloo, Ontario, Canada, N2L 3G1. {a5akhtar,stevenw cnielsen}@uwaterloo.ca

can be represented as,

$$\begin{aligned}
\dot{x}_1 &= x_4 + x_5 S_1 T_2 + x_6 C_1 T_2 \\
\dot{x}_2 &= x_5 C_1 - x_6 S_1 \\
\dot{x}_3 &= \sec(x_2)(x_5 S_1 + x_6 C_1) \\
\dot{x}_4 &= -((I_z - I_y)/I_x) x_5 x_6 - (k_r x_4 / I_x) + (1/I_x)\tau_p \\
\dot{x}_5 &= -((I_x - I_z)/I_y) x_4 x_6 - (k_r x_5 / I_y) + (1/I_y)\tau_q \\
\dot{x}_6 &= -((I_y - I_x)/I_z) x_4 x_5 - (k_r x_6 / I_z) + (1/I_z)\tau_r \\
\dot{x}_7 &= x_{10} \\
\dot{x}_8 &= x_{11} \\
\dot{x}_9 &= x_{12} \\
\dot{x}_{10} &= (-k_t x_{10}/m) + (1/m)(C_1 S_2 C_3 + S_1 S_3)\tau_f \\
\dot{x}_{11} &= (-k_t x_{11}/m) + (1/m)(C_1 S_2 S_3 - S_1 C_3)\tau_f \\
\dot{x}_{12} &= (-k_t x_{12}/m) + g - (1/m)(C_1 C_2)\tau_f,
\end{aligned} \tag{1}$$

where, I_x, I_y, I_z represent inertia, m represents mass of the quadrotor, k_t and k_r represent the translational and rotational drag coefficients and are assumed to be constant in all directions for simplicity. The control inputs are represented by τ_p, τ_q, τ_r, and τ_f. The acceleration due to gravity is represented by g.

The forces and torques in the body axis are given by

$$\begin{bmatrix} \tau_f \\ \tau_p \\ \tau_q \\ \tau_r \end{bmatrix} = \begin{bmatrix} 1 & 1 & 1 & 1 \\ 0 & -l & 0 & l \\ -l & 0 & l & 0 \\ d & -d & d & -d \end{bmatrix} \begin{bmatrix} f_1 \\ f_2 \\ f_3 \\ f_4 \end{bmatrix}, \tag{2}$$

where, l is the distance from the center of mass to the rotors, d is the ratio between the drag and the thrust coefficients of the blade and f_i for $i = \{1, 2, 3, 4\}$ are the forces generated by the four rotors of the quadrotor.

III. Fault Tolerant Control System

Informally, a fault tolerant control (FTC) system is a system that can maintain stability in the presence of particular faults. The fault tolerant path following control considered in this paper is based on the assumption that path following must be maintained in the event one of the rotors no longer provides any thrust or moment. Such a scenario generally occurs when a rotor collides with a static object in the environment, causing the rotor blade to break, a propeller loss, or an electrical failure. During typical operation the quadrotor flies in a fault-free fashion and the path following controller [5] designed in our previous work can be used. However, when a failure occurs, the goal of path following becomes more challenging because the requirements of path invariance and pre-defined velocity profile tracking must be maintained using only three motors. The controller is of practical importance because it allows a quadrotor to recover from a single rotor failure and maintain path invariance at the expense of independent control over yaw angle. The result is a vehicle that spins about its body z-axis while travelling along the path. The rate at which the yaw varies can be bounded, allowing for safe operation in the presence of such a failure.

Without loss of generality, assume the second motor M_2 fails due to collision. A fault diagnosis system detects a severe effect on the vehicle roll control, and triggers the switch from the fault free state to the faulty state and turns off M_2 completely. The new control inputs are τ_f, τ_q, τ_r, and (2) becomes

$$\begin{bmatrix} \tau_f \\ \tau_p \\ \tau_q \\ \tau_r \end{bmatrix} = \begin{bmatrix} 1 & 1 & 1 \\ 0 & 0 & l \\ -l & l & 0 \\ d & d & -d \end{bmatrix} \begin{bmatrix} f_1 \\ f_3 \\ f_4 \end{bmatrix}. \tag{3}$$

The expression $\tau_p = l f_4 = \tau_f - \frac{\tau_r}{d}$ can be substituted into the quadrotor model (1). As in the fault free case, the output of the quadrotor is the position of the center of gravity of the quadrotor in the inertial frame

$$y(x) = h(\chi) = \begin{bmatrix} x_7 & x_8 & x_9 \end{bmatrix}^\top. \tag{4}$$

IV. Problem Statement

Most commonly, the goal in path following is to force the output of the given system to converge and move along a path. The path is generally not pre-assigned a timing law which makes a path different from a trajectory.

Consider a regular, smooth curve $\gamma \subset \mathbb{R}^3$ in the quadrotor's output space. Let $\sigma : \mathbb{D} \to \mathbb{R}^3$ be a unit-speed parameterization of γ, i.e., $\gamma = \sigma(\mathbb{D})$. For non-closed curves $\mathbb{D} = \mathbb{R}$. For closed curves of length $L > 0$, $\mathbb{D} = \mathbb{R} \bmod L$ and σ is L-periodic, i.e., for any $\lambda \in \mathbb{D}$, $\sigma(\lambda + L) = \sigma(L)$. Similar to our previous work [5], the following assumptions are imposed.

Assumption 1. *The curve $\gamma \subset \mathbb{R}^3$ is a one-dimensional embedded submanifold. There exists a smooth map $s : \mathbb{R}^3 \to \mathbb{R}^2$ so that $\gamma = s^{-1}(0)$ with $\operatorname{rank}(ds_y) = 2$ for all $y \in \gamma$.*

The path γ can be lifted to the state space

$$\Gamma := \left\{ x \in \mathbb{R}^{12} : s_1(h(x)) = s_2(h(x)) = 0 \right\}.$$

Forcing $y \to \gamma$ is equivalent to making $x \to \Gamma$. However, in general Γ can not be made invariant, so we seek to stabilize a subset of Γ [5].

Given a path that satisfies Assumption 1, we seek a smooth dynamic feedback law

$$\begin{aligned}
\dot{\zeta} &= \mathcal{A}(x, \zeta) + \mathcal{B}(x, \zeta) u \\
\overline{u} &= \mathcal{C}(x, \zeta) + \mathcal{D}(x, \zeta) u,
\end{aligned} \tag{5}$$

with[1] $\zeta \in \mathbb{R}^{\widetilde{q}}$, $u \in \mathbb{R}^3$ and an open subset of initial conditions in a neighborhood of the lift of the path, such that the quadrotor with one damaged rotor meets the following goals,

- **G1** The system asymptotically approaches the path, $\|h(x(t))\|_\gamma \to 0$ as $t \to \infty$.
- **G2** The zero level set $s(y)$ is output invariant for all $t \geq 0$.
- **G3** On the path, the system follows a desired speed profile along the curve.
- **G4** The body rates p, q, r remain bounded, i.e., $|p| < \infty$, $|q| < \infty$, and $|r| < \infty$ for all $t \geq 0$.

[1]The dimension $\widetilde{q}$ of the controller state ζ is not fixed *a priori*.

G5 The system does not spin at unbounded rate about its axis, i.e., $|\dot{\psi}| < \infty$ for all $t \geq 0$.

A. Dynamic Extension

As discussed in [5], [12]–[14], the largest controlled invariant submanifold $\Gamma^\star$ contained in Γ is called the path following manifold. The path following manifold is key to solving the path following problem because by a suitable choice of the control input all the associated trajectories can be made to remain on the desired path. Making $\Gamma^\star$ attractive and invariant implies the fulfilment of **G1** and **G2**. In order to find $\Gamma^\star$ we first define

$$\alpha = \begin{bmatrix} \alpha_1(x) \\ \alpha_2(x) \end{bmatrix} := s \circ h(x) = \begin{bmatrix} s_1 \circ h(x) \\ s_2 \circ h(x) \end{bmatrix}. \quad (6)$$

With this definition we have that $\Gamma = \alpha^{-1}(0)$ and as a result, we can apply the zero dynamics algorithm [15] to the function α to obtain a local characterization of $\Gamma^\star$.

Since the faulted quadrotor has only three inputs it is natural to augment the function (6) with one additional function to make the number of output functions equal to the number of control inputs and then check the relative degree of the system with respect to the augmented output. To this end let $\pi(x_7, x_8, x_9)$ be any smooth real-valued function. It is easy to show, see [5], that the "virtual" output $\bar{y} = (\alpha, \pi(x))$ fails to yield a well-defined relative degree for the system (1) because the decoupling matrix is always rank deficient.

This problem is overcome by delaying the appearance of the control input τ_f with the help of two integrators, which are included through two additional states $x_{13} := \tau_f$ and $x_{14} := \dot{\tau}_f$. Let $u_d = \ddot{\tau}_f$ and $u = \text{col}(u_d, u_q, u_r) \in \mathbb{R}^3$, where $u_r := \tau_r$ and $u_q := \tau_q$. With a slight abuse of notation we write the extended model compactly as $\dot{x} = f(x) + \sum_{i=1}^{3} g_i(x)u_i$. As in [5], applying the zero dynamics algorithm to the output (6) and the extended system yields the path following manifold

$$\Gamma^\star = \left\{ x \in \mathbb{R}^{14} : L_f^i \alpha(x) = 0, i = 0, 1, 2, 3, 4 \right\}. \quad (7)$$

V. Path Following Controller Design

In this work the general approach for solving path following problem [5], [12], [14] is applied to a quadrotor with a failed rotor. Unlike previous cases [5], [14] where the system was fully feedback linearized, in this paper only a partially feedback linearized system is obtained. The system is therefore not differentially flat with our particular choice of output functions. We now refine the definition of π in the virtual output $\hat{y}$ of Section IV-A by choosing a function similar to the one used in the fault free case [5]. Let $\gamma_\epsilon \subset \mathbb{R}^3$ be a tubular neighbourhood of the path γ and define the map

$$\begin{aligned} \varpi : &\gamma_\epsilon \to \mathbb{D} \\ &y \mapsto \arg \inf_{\lambda \in \mathbb{D}} \|y - \sigma(\lambda)\|. \end{aligned} \quad (8)$$

The above function is smooth so long as γ_ϵ is a sufficiently small "tube" around the curve γ. With these definitions and Assumption 1, we refine the "virtual output" function $\hat{y}$ to be

$$\hat{y} = \begin{bmatrix} \alpha_1(x_7, x_8, x_9) \\ \alpha_2(x_7, x_8, x_9) \\ \pi(x_7, x_8, x_9) \end{bmatrix} = \begin{bmatrix} s_1 \circ h(\chi) \\ s_2 \circ h(\chi) \\ \varpi \circ h(\chi) \end{bmatrix}. \quad (9)$$

The next two results are presented to support our claim that the extended system has a well-defined vector relative degree at each point of the path following manifold. The first is presented without proof as it is the well known triple product result from linear algebra.

Lemma V.1 ([16]). *If v_1,v_2,v_3 are linearly independent vectors in $\mathbb{R}^3$ then $\langle v_1, (v_2 \times v_3) \rangle \neq 0$.*

Let $d_\chi \alpha_i := \text{col}(\frac{\partial \alpha_i}{\partial x_7}, \frac{\partial \alpha_i}{\partial x_8}, \frac{\partial \alpha_i}{\partial x_9})$ for $i = \{1, 2\}$ and $\sigma' := \text{col}(\frac{\partial \sigma}{\partial \lambda}, \frac{\partial \sigma}{\partial \lambda}, \frac{\partial \sigma}{\partial \lambda})$.

Lemma V.2. *Let α_1 and α_2 be as defined in (6). Then, for all $\chi \in \gamma$, $\text{span}\{d_\chi \alpha_1, d_\chi \alpha_2, \sigma'\} = \mathbb{R}^3$.*

Proof. We first show that each of the vectors $d_\chi \alpha_1, d_\chi \alpha_2, \sigma'$ are non zero. By assumption, σ is regular which means $\sigma' \neq 0$. Also by Assumption 1, at each $y \in \gamma$, ds_y has rank two. Since $dh_x = I$ this shows, using the chain rule, that at each $\chi^\star \in \Gamma$, $d_\chi \alpha$ has rank two. Since σ' is a tangent vector and $d_\chi \alpha_1, d_\chi \alpha_2$ are non-zero gradient vectors, we conclude that $\text{span}\{d_\chi \alpha_1, d_\chi \alpha_2, \sigma'\} = \mathbb{R}^3$ as claimed. □

We claim that state x_{13}, which represents τ_f, the combined thrust of all the rotors can not be zero in reasonable flight conditions. In fact, x_{13} is zero if an only if all the rotors of the system stop spinning at the same time. Therefore, for all practical purposes $x_{13} \neq 0$ is a valid assumption. Moreover, we assume that in this work the system does not encounter gimbal lock situation[2], i.e., $\phi = \theta \neq \pm 90^0$.

Lemma V.3. *The extended model of the quadrotor with output (9) yields a well-defined vector relative degree of $\{4, 4, 4\}$ at each point on $\Gamma^\star \cap \{x \in \mathbb{R}^{14} : x_{13} \neq 0\}$.*

Proof. Let $x^\star \in \Gamma^\star \cap \{x \in \mathbb{R}^{14} : x_{13} \neq 0\}$ be arbitrary. By definition of Γ, and since $\Gamma^\star \subseteq \Gamma$, the output $h(x^\star)$ is on the path γ. Let $\lambda^\star \in \mathbb{D}$ be such that $h(x^\star) = \sigma(\lambda^\star)$. By the definition of vector relative degree we must show that

$$L_{g_i} L_f^j \pi(x) = L_{g_i} L_f^j \alpha_k(x) \equiv 0$$

for $i \in \{1, 2, 3\}$, $j \in \{0, 1, 2\}$, $k \in \{1, 2\}$ in a neighbourhood of $x^\star$ and that the 3×3 decoupling matrix

$$D(x^\star) = \begin{bmatrix} L_{g_1} L_f^3 \alpha_1(x^\star) & L_{g_2} L_f^3 \alpha_1(x^\star) & L_{g_3} L_f^3 \alpha_1(x^\star) \\ L_{g_1} L_f^3 \alpha_2(x^\star) & L_{g_2} L_f^3 \alpha_2(x^\star) & L_{g_3} L_f^3 \alpha_2(x^\star) \\ L_{g_1} L_f^3 \pi(x^\star) & L_{g_2} L_f^3 \pi(x^\star) & L_{g_3} L_f^3 \pi(x^\star) \end{bmatrix}, \quad (10)$$

is non-singular. It is easy to check, by direct computations, that the first condition holds and

$$\det(D(x)) = \frac{l(x_{13})^2}{I_x I_y m^3 d} \langle -d_\chi \alpha_1, (d_\chi \alpha_2 \times \sigma') \rangle. \quad (11)$$

[2]The singularity associated with gimbal lock is due to our choice of parameterization, i.e., Euler angles, on $\mathsf{SO}(3)$.

The determinant goes to zero if and only if any term in the numerator of (11) is zero or any term in the denominator is infinity. The terms I_x, I_y, d, l and m are finite constants. By assumption, at $x^\star \in \Gamma^\star \cap \{x \in \mathbb{R}^{14} : x_{13} \neq 0\}$, the combined thrust $x_{13} \neq 0$. By Lemma V.2, $\text{span}\{d_\chi\alpha_1, d_\chi\alpha_2, \sigma'\}(x^\star) = \mathbb{R}^3$ and therefore, by Lemma V.1 $\langle -d_\chi\alpha_1, (d_\chi\alpha_2 \times \sigma')\rangle \neq 0$ at $x^\star$. Thus we have shown that for any $x^\star \in \Gamma^\star \cap \{x \in \mathbb{R}^{14} : x_{13} \neq 0\}$, $\det(D(x^\star)) \neq 0$, therefore the extended system has a well defined vector relative degree at $x^\star$. □

The extended system has a well defined vector relative degree of $\{4,4,4\}$, which implies that the dimension of the internal dynamics is $14-(4+4+4)=2$. Two additional functions are needed to define a complete coordinate transformation.

Corollary V.4. *Let $x^\star \in \Gamma^\star \backslash \{x \in \mathbb{R}^{14} : x_1 \pm 90^0,\ x_{13} \neq 0\}$. There exists a neighbourhood $U \subset \mathbb{R}^{14}$ containing $x^\star$ such that the mapping $T : U \subset \mathbb{R}^{14} \to T(U) \subset \mathbb{R}^{14}$, defined by*

$$\begin{bmatrix} \xi_{ji} \\ \eta_i \\ \mu_k \end{bmatrix} = T(x) = \begin{bmatrix} L_f^{i-1}\alpha_j(x) \\ L_f^{i-1}\pi(x) \\ \mu(x) \end{bmatrix}, \tag{12}$$

for $i \in \{1,2,3,4\}$, $j \in \{1,2\}$ and $k \in \{1,2\}$, is a diffeomorphism.

Proof. The choice of $(\xi, \eta) \in \mathbb{R}^{12}$ is clear from (12). However, the relative degree of the extended system is 2 less than the dimension of the state space. Therefore we must select two additional real-valued functions μ_1, μ_2 to complete the definition of T. The distribution $G_0(x) := \text{span}\{g_1, g_2, g_3\}(x)$ is constant and therefore involutive. By [15, Proposition 5.1.2] there exist real-valued functions μ_1 and μ_2 whose differentials belong to the annihilator of $G_0(x)$ and complete the coordinate transformation T. Two possible choices are

$$\begin{aligned} \mu_1 &:= x_3, \\ \mu_2 &:= -\frac{-x_4}{I_z} - \frac{Lx_6}{2I_x d}. \end{aligned} \tag{13}$$

With the above choice of μ_1 and μ_2 it is sufficient to check the rank of the 14×14 Jacobian matrix. The determinant of Jacobian matrix $\frac{dT}{dx}$ is given by

$$\frac{-l(x_{13})^4 C_1}{2I_x m^6 d}\langle -d_\chi\alpha_1, (d_\chi\alpha_2 \times \sigma')\rangle. \tag{14}$$

By Lemma V.3, Equation (14) equals zero at $x^\star \in \Gamma^\star \cap \{x \in \mathbb{R}^{14} : x_{13} \neq 0\}$ if and only if $C_1 = 0$. However, by hypothesis, the gimbal lock condition $\phi = \theta = \pm 90^0$ does not hold at $x^\star$. Therefore, the Jacobian of T is non-singular in a neighbourhood of $x^\star$ and T is a local diffeomorphism. □

Using the coordinate transformation T from Corollary V.4, the system is differentially equivalent in a neighbourhood of $x^\star$ to

$$\begin{aligned} \dot{\xi}_{ij} &= \xi_{ij+1} \\ \dot{\eta}_j &= \eta_{j+1} \\ \dot{\xi}_{14} &= L_f^4\alpha_1 + L_{g_1}L_f^3\alpha_1 u_f\big|_{x=T^{-1}(\eta,\xi,\mu)} \\ \dot{\xi}_{24} &= L_f^4\alpha_2 + L_{g_2}L_f^3\alpha_2 u_r\big|_{x=T^{-1}(\eta,\xi,\mu)} \\ \dot{\eta}_4 &= L_f^4\pi + L_{g_3}L_f^3\pi u_q\big|_{x=T^{-1}(\eta,\xi,\mu)} \\ \dot{\mu}_k &= b_k(\eta,\xi,\mu)\big|_{x=T^{-1}(\eta,\xi,\mu)} \end{aligned} \tag{15}$$

for $i \in \{1,2\}$, $j \in \{1,2,3\}$, $k \in \{1,2\}$ and where b_k are smooth nonlinear functions. The structure of (15) suggests the feedback transformation

$$\begin{bmatrix} u_f \\ u_r \\ u_q \end{bmatrix} := D^{-1}(x)\left(\begin{bmatrix} -L_f^4\alpha_1 \\ -L_f^4\alpha_2 \\ -L_f^4\pi \end{bmatrix} + \begin{bmatrix} v^{\xi_1} \\ v^{\xi_2} \\ v^{\eta} \end{bmatrix}\right), \tag{16}$$

where $(v^{\xi_1}, v^{\xi_2}, v^\eta)$ are auxiliary control inputs. By Lemma V.3 the feedback transformation (16) is well-defined in a neighborhood of every $x^\star \in \Gamma^\star \cap \{x \in \mathbb{R}^{14} : x_{13} \neq 0\}$. Thus in a neighborhood of $x^\star$, the closed-loop system is reduced to 3 decoupled chains of integrators and the nonlinear internal dynamics of the system.

After applying the coordinate and feedback transformations (12), (16) to the extended system the auxiliary controller design is straight forward for the linear subsystems. A linear controller similar to [5] can be designed to stabilize the origin of the ξ. Similarly a linear controller can be designed for the $\eta-$subsystem to satisfy **G3**.

VI. Internal Dynamics

The μ-subsystem represents the internal dynamics

$$\begin{aligned} \dot{\mu}_1(\eta,\xi,\mu) &= \sec(x_2)(x_6C_1 + x_5S_1)\big|_{x=T^{-1}(\eta,\xi,\mu)}, \\ \dot{\mu}_2(\eta,\xi,\mu) &= -\frac{0.5lx_{13}}{I_xI_z} + \frac{lk_rx_6}{2I_xI_zd} \\ &\quad + \frac{k_rx_4 + x_5x_6(I_x - I_z)}{I_xI_z}\Big|_{x=T^{-1}(\eta,\xi,\mu)}. \end{aligned} \tag{17}$$

In order to prove boundedness of the internal dynamics (Lemma VI.3), we need the following preliminary results. We first analyze the stability of the set of differential equations involving the dynamics of the body rates from when the control inputs are set to zero.

Lemma VI.1. *The origin $(x_4, x_5, x_6) = (0,0,0)$ of*

$$\begin{aligned} \dot{x}_4 &= -((I_z - I_y)/I_x)x_5x_6 - (k_rx_4)/I_x \\ \dot{x}_5 &= -((I_x - I_z)/I_y)x_4x_6 - (k_rx_5)/I_y \\ \dot{x}_6 &= -((I_y - I_x)/I_z)x_4x_5 - (k_rx_6)/I_z. \end{aligned} \tag{18}$$

is globally exponentially stable.

Proof. We assume, without the loss of generality, that $I_x \geq I_y \geq I_z$, and let

$$\begin{aligned} a_1 &:= \frac{I_y - I_z}{I_x}, \quad a_2 := \frac{I_x - I_z}{I_y}, \quad a_3 := \frac{I_x - I_y}{I_z} \\ k_4 &:= \frac{k_r}{I_x}, \quad k_5 := \frac{k_r}{I_y}, \quad k_6 := \frac{k_r}{I_z}. \end{aligned}$$

If $I_x \geq I_y \geq I_z$ does not hold, a_1, a_2, a_3 can be redefined, so that these constants are non-negative. With these definitions, (18) becomes

$$\begin{aligned} \dot{x}_4 &= a_1 x_5 x_6 - k_4 x_4 \\ \dot{x}_5 &= -a_2 x_4 x_6 - k_5 x_5 \\ \dot{x}_6 &= a_3 x_4 x_5 - k_6 x_6. \end{aligned} \tag{19}$$

Equation (19) can be written as $\dot{\overline{x}} = \overline{f}(\overline{x})$, for $\overline{x} := \text{col}(x_4, x_5, x_6)$. Choose as a candidate Lyapunov function $V : \mathbb{R}^3 \to \mathbb{R}$

$$V(\overline{x}) = \overline{x}^\top P \overline{x} := p_1 x_4^2 + p_2 x_5^2 + p_3 x_6^2 \tag{20}$$

where $P := \text{diag}\,(p_1, p_2, p_3)$. If p_1, p_2, p_3 are positive then V is a positive definite quadratic form. The Lie derivative of V along the vector field (19) is

$$\begin{aligned} L_{\overline{f}} V = &\, 2 x_4 x_5 x_6 \left(a_1 p_1 - a_2 p_2 + a_3 p_3\right) \\ &- 2 \overline{x}^\top \text{diag}\,(k_4 p_1, k_5 p_2, k_6 p_3) \overline{x}. \end{aligned}$$

Now choose $p_1, p_2, p_3 > 0$ so that $a_1 p_1 - a_2 p_2 + a_3 p_3 = 0$. This is always possible, for example $p_1 = I_x$, $p_2 = I_y$, $p_3 = I_z$ works. In summary we have that

(i) For all $\overline{x} \in \mathbb{R}^3$,

$$\min\{p_1, p_2, p_3\} \|\overline{x}\|_2^2 \leq V(\bar{x}) \leq \max\{p_1, p_2, p_3\} \|\overline{x}\|_2^2$$

(ii) For all $\overline{x} \in \mathbb{R}^3$,

$$\begin{aligned} L_{\overline{f}} V &= -2 \overline{x}^\top \text{diag}\,(k_4 p_1, k_5 p_2, k_6 p_3) \overline{x} \\ &\leq -2 \min\{k_4 p_1, k_5 p_2, k_6 p_3\} \|\overline{x}\|_2^2 \\ &= -2 \min\{k_4 p_1, k_5 p_2, k_6 p_3\} \frac{\max\{p_1, p_2, p_3\}}{\max\{p_1, p_2, p_3\}} \|\overline{x}\|_2^2 \\ &\leq -2 \frac{\min\{k_4 p_1, k_5 p_2, k_6 p_3\}}{\max\{p_1, p_2, p_3\}} V(\overline{x}) \end{aligned}$$

Conditions (i) and (ii) imply, by [17, Theorem 3.1], that $\overline{x} = 0$ is globally exponentially stable.

□

Next we analyze the stability the body rate equations and show that they are input-to-state stable (ISS-stable) [18]. Let $k_7 := l/2I_x$, $k_8 := -1/dI_x$, $k_9 := 1/I_y$, $k_{10} := 1/I_z$.

Lemma VI.2. *The system* (21)

$$\begin{aligned} \dot{x}_4 &= a_1 x_5 x_6 - k_4 x_4 + k_7 x_{13} + k_8 u_2 \\ \dot{x}_5 &= -a_2 x_4 x_6 - k_5 x_5 + k_9 u_3 \\ \dot{x}_6 &= a_3 x_4 x_5 - k_6 x_6 + k_{10} u_2, \end{aligned} \tag{21}$$

is input-to-state stable.

Proof. To be consistent with the notation we used for (19), write this system as

$$\dot{\overline{x}} = \overline{f}(\overline{x}) + B\overline{w}$$

where

$$\overline{w} := \begin{bmatrix} x_{13} \\ u_r \\ u_q \end{bmatrix}, B := \begin{bmatrix} k_7 & k_8 & 0 \\ 0 & 0 & k_9 \\ 0 & k_{10} & 0 \end{bmatrix}.$$

To prove that the system (21) is ISS-stable we show that the function (20) is an ISS-Lyapunov function. As in the proof of Lemma VI.1, choose $p_1, p_2, p_3 > 0$ so that $a_1 p_1 - a_2 p_2 + a_3 p_3 = 0$. Then $Q := \text{diag}\,(k_4 p_1, k_5 p_2, k_6 p_3)$ and we have

$$\begin{aligned} \dot{V} &= -2\overline{x}^\top Q \overline{x} + 2\overline{x}^\top P B \overline{w} \\ &= -2(1-\theta)\overline{x}^\top Q \overline{x} - 2\theta \overline{x}^\top Q \overline{x} + 2\overline{x}^\top Q B \overline{w}, \ (\forall\, \theta \in (0,1)) \\ &\leq -2(1-\theta)\overline{x}^\top Q \overline{x} - 2\theta \min\{k_4 p_1, k_5 p_2, k_6 p_3\} \|\overline{x}\|_2^2 \\ &\quad + 2\overline{x}^\top Q B \overline{w} \\ &\leq -2(1-\theta)\overline{x}^\top Q \overline{x} - 2\theta \min\{k_4 p_1, k_5 p_2, k_6 p_3\} \|\overline{x}\|_2^2 \\ &\quad + 2\|\overline{x}\|_2 \|Q\|_2 \|B\|_2 \|\overline{w}\|_2. \end{aligned}$$

Thus

$$\forall\ \|\overline{x}\|_2 \geq \frac{\|Q\|_2 \|B\|_2}{\theta \min\{k_4 p_1, k_5 p_2, k_6 p_3\}} \|\overline{w}\|_2,$$

$$\dot{V} \leq -(1-\theta)\overline{x}^\top Q \overline{x}$$

where $\theta \in (0,1)$. This shows, by [19, Theorem 4.19], that (21) is ISS stable. □

In summary, by Lemmas VI.1 and VI.2 we have shown that the body rates x_4, x_5, x_6 are bounded.

Lemma VI.3. *If the control inputs u_f, u_r, u_q of the quadrotor are bounded and the quadrotor avoids the gimbal lock condition ($x_1 = x_2 = \pm 90^0$), then $\dot{\mu}_1$ and $\dot{\mu}_2$ in (17) are bounded. Moreover, μ_2 is bounded.*

Proof. By Lemma VI.2 we have shown that for any bounded inputs, the body rates x_4, x_5, x_6 are bounded. By hypothesis the system is bounded away from Euler angle singularities ($x_1 = x_2 = \pm 90^0$). From the expressions (17) we have that

$$\begin{aligned} |\dot{\mu}_1| &\leq \sec(x_2)\left(|x_5| + |x_6|\right), \\ |\dot{\mu}_2| &\leq \frac{l k_r}{2 d I_x I_z} |x_6| + \frac{l}{2 I_x I_z} |x_{13}| + \frac{k_r}{I_x I_z} |x_4| \\ &\quad + \frac{I_z - I_x}{I_x I_z} |x_5||x_6|, \\ |\mu_2| &\leq \frac{1}{I_z} |x_4| - \frac{l}{2 d I_x} |x_6|, \end{aligned} \tag{22}$$

which is bounded because the body rates are bounded and $x_2 \neq 0$ during the flight. □

In summary, all the goals **G1-G5** are achieved. It is interesting to note that the internal state μ_1 which represent the yaw angle may become unbounded. This implies that the quadrotor is spinning about its body z-axis while traveling along the path, which is not surprising as there is an imbalance in torques that results when one of the four rotors fails. However, we have shown that rate at which the quadrotor spins $\dot{\mu}_1 = \dot{\psi}$ is bounded, which is a result of the rotational drag term about the body z-axis that resists overly fast rotation, regardless of the path traveled.

VII. Simulation

For simulation purposes, it is assumed that the quadrotor has a mass of $m = 4.493$ kg, and inertias $I_x = I_y = 0.177$ kg.m^2 and $I_z = 0.344$ kg.m^2, a length $l = 0.1$ m and acceleration due to gravity is $g = 9.8$ m/sec^2. The initial position of the quadrotor is indicated by a solid dot. The values of k_t and k_r used in the simulation are taken from the rotational and translational drag models presented in [20], [21].

We consider a curve at varying height given by $\sin(x_7) + 3$ units represented as $\sigma : \mathbb{R} \to \mathbb{R}^3$, $\lambda \mapsto \text{col}(\lambda, \cos(\lambda), \sin(\lambda) + 3)$. The implicit representation of the same curve is given by $\gamma = \{s_1(y) = s_2(y) = 0\}$, where $s_1(y) = y_2 - cos(y_1) = 0$ and $s_2 = y_3 + \sin(y_1) - 3$. The quadrotor is initialized at $(x_7, x_8, x_9) = (0, 0.9, 0)$. The results are shown in Figure 1. While following the path γ

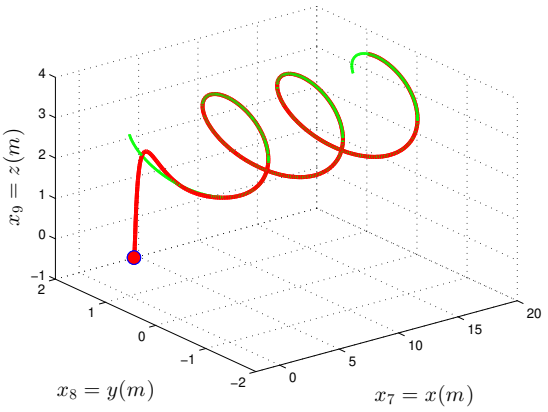

Fig. 1. The path followed by the quadrotor is represented by a bold line and the desired path is represented by a dashed line. The initial position of the quadrotor is represented by a solid dot.

the quadrotor is following the curve at a desired constant speed of 0.3 m/sec, as presented in Figure 2. In Figure 3 the

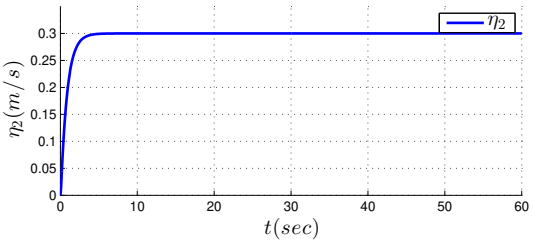

Fig. 2. The quadrotor is traversing the curve at the desired velocity of 0.3 m/sec.

internal state $\dot{\mu}_1$ is shown. It represents the rate at which the quadrotor is spinning about its axis which remains bounded.

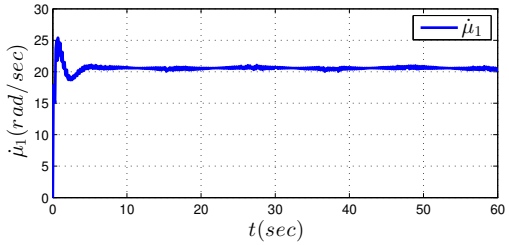

Fig. 3. The yaw rate $\dot{\mu}_1$ remains bounded as the quadrotor traverses the desired path.

References

[1] A. Benallegue, A. Mokhtari, and L. Fridman, "Feedback linearization and high order sliding mode observer for a quadrotor uav," in *Variable Structure Systems, 2006. VSS'06. International Workshop on*, June 2006, pp. 365 –372.

[2] H. Voos, "Nonlinear control of a quadrotor micro-UAV using feedback-linearization," in *Mechatronics, 2009. ICM 2009. IEEE International Conference on*, April 2009, pp. 1–6.

[3] D. Lee, H. Jin Kim, and S. Sastry, "Feedback linearization vs. adaptive sliding mode control for a quadrotor helicopter," *International Journal of Control, Automation and Systems*, vol. 7, no. 3, pp. 419–428, 2009.

[4] T. Madani and A. Benallegue, "Control of a quadrotor mini-helicopter via full state backstepping technique," in *Decision and Control, 2006 45th IEEE Conference on*, Dec. 2006, pp. 1515–1520.

[5] A. Akhtar, S. L. Waslander, and C. Nielsen, "Path following for a quadrotor using dynamic extension and transverse feedback linearization," in *Decision and Control (CDC), 2012 IEEE 51st Annual Conference on*, Dec. 2012, pp. 3551 –3556.

[6] T. Li, "Nonlinear and fault-tolerant control techniques for a quadrotor unmanned aerial vehicle," Concordia University, Tech. Rep., 2011.

[7] Y. Zhang and A. Chamseddine, *Fault Tolerant Flight Control Techniques with Application to a Quadrotor UAV Testbed, Automatic Flight Control Systems*. InTech, 2012.

[8] H. Jiang, Y. Yu, X. Ding, and J. Zhu, "A fault tolerant control strategy for quadrotor UAVs based on trajectory linearization approach," in *Mechatronics and Automation (ICMA), 2012 International Conference on*, Aug. 2012, pp. 1174–1179.

[9] A. Freddi, A. Lanzon, and S. Longhi, "A feedback linearization approach to fault tolerance in quadrotor vehicles," pp. 5413–5418, Aug. 2011.

[10] D. Lee and H. Kim, "Adaptive visual servo control for a quadrotor helicopter," in *Control Automation and Systems (ICCAS), 2010 International Conference on*, Oct. 2010, pp. 1049–1052.

[11] G. M. Hoffmann, H. Huang, S. L. Waslander, and C. J. Tomlin, "Precision flight control for a multi-vehicle quadrotor helicopter testbed," *Control Engineering Practice*, vol. 19, no. 9, pp. 1023–1036, September 2011.

[12] C. Nielsen, C. Fulford, and M. Maggiore, "Path following using transverse feedback linearization: Application to a maglev positioning system," *Automatica*, vol. 46, no. 3, pp. 585–590, March 2010.

[13] L. Consolini, M. Maggiore, C. Nielsen, and M. Tosques, "Path following for the PVTOL aircraft," *Automatica*, vol. 46, no. 8, pp. 1284–1296, August 2010.

[14] A. Akhtar and C. Nielsen, "Path following for a car-like robot using transverse feedback linearization and tangential dynamic extension," in *Decision and Control and European Control Conference, CDC-ECC 2011. 50th IEEE Conference on*, Dec. 2011, pp. 7949 –7979.

[15] A. Isidori, *Nonlinear Control Systems*. Secaucus, NJ, U.S.A: Springer-Verlag New York, Inc., 1995.

[16] G. Strang, *Linear Algebra and its applications*. 111 Fifth Avenue, New York, New York 10003: Academic Press, INC, 1976.

[17] W. Haddad and V. Chellaboina, *Nonlinear Dynamical Systems and Control*. Prentice University Press, 2008.

[18] E. Sontag, "Smooth stabilization implies coprime factorization," *IEEE Transactions on Automatic Control*, vol. 34, no. 4, pp. 435–443, 1989.

[19] H. K. Khalil, *Nonlinear systems*, 3rd ed. Prentice Hall, 2002.

[20] *The Role of Propeller Aerodynamics in the Model of a Quadrotor UAV*, Budapest, 2009.

[21] J. Meyer, A. Sendobry, S. Kohlbrecher, U. Klingauf, and O. von Stryk, "Comprehensive simulation of quadrotor uavs using ros and gazebo," in *3rd Int. Conf. on Simulation, Modeling and Programming for Autonomous Robots (SIMPAR)*, 2012.